Revisiting an old concept: the coupled oscillator model for VCD. Part 1: The generalised coupled oscillators mechanism and its intrinsic connection to the strength of VCD signals

Valentin Paul Nicu[1]

Van 't Hoff Institute for Molecular Sciences, University of Amsterdam, Science Park 904, 1098 XH Amsterdam, The Netherlands

Electronic Supplementary Information

[1]email: V.P.Nicu@uva.nl, vp.nicu@gmail.com

1 GCO analysis: (R)-2,2'-spirobi[indene]-1,1'(3H,3'H)-dione

This section describes the GCO analysis performed for all normal modes of the molecular complex formed between one (R)-2,2'-spirobi[indene]-1,1'(3H,3'H)-dione molecule and two chloroform solvent molecules.

When analysing different types of normal modes, different definitions of the GCO fragments **A**, **B** and **R** need to be used, viz. different types of normal modes involve movements of different groups of atoms. From the perspective of the GCO analysis one can distinguish between four main types of normal modes: I) modes localised entirely on the solute molecule, II) modes localised entirely on the solvent molecules, III) modes that are localised on the solute and solvent molecules, and IV) modes that involve strong movements of the central C atom. Fig. 1 shows the definitions of the molecular fragments **A**, **B** and **R** used in the GCO analysis of these four types of modes. The results of the GCO analysis are listed in Tables I and II.

[Figure 1 about here.]

It should also be noted that Eq. 19 in the manuscript is properly defined only when $R_{01}^{\mathbf{CO}}$ is not zero. If $R_{01}^{\mathbf{CO}}$ is zero or very small, there is no reason to consider $R_{01}^{\mathbf{COC}}$ as a correction for $R_{01}^{\mathbf{CO}}$. Since many modes have small $R_{01}^{\mathbf{CO}}$ terms and thus very large $a(j)$ factors, this information is not shown in Tables I and II.

[Table 1 about here.]

[Table 2 about here.]

2 GCO analysis: dehydroquinidine

For simplicity, a GCO analysis was performed for DHQD by dividing the molecules in only two fragments. In this case, the expression describing the fragment decomposition of the rotational strength becomes:

$$R_{01}(j) = -i \cdot \vec{E}_{01}(j) \cdot \vec{M}_{10}(j) = R_{01}^{\mathbf{IF}}(j) + R_{01}^{\mathbf{GCO}}(j) \tag{1}$$

where:

$$R_{01}^{\mathbf{IF}}(j) = -i \cdot \left[\vec{E}_{01}^{\mathbf{A}}(j) \cdot \vec{M}_{10}^{\mathbf{A}}(j) + \vec{E}_{01}^{\mathbf{B}}(j) \cdot \vec{M}_{10}^{\mathbf{B}}(j)\right] \tag{2}$$

$$R_{01}^{\mathbf{GCO}}(j) = -i \cdot \left[\vec{E}_{01}^{\mathbf{A}}(j) \cdot \vec{M}_{10}^{\mathbf{B}}(j) + \vec{E}_{01}^{\mathbf{B}}(j) \cdot \vec{M}_{10}^{\mathbf{A}}(j)\right] \tag{3}$$

As before, $R_{01}^{\mathbf{IF}}(j)$ represents the contribution to the total rotational strengths from the individual fragments, whereas $R_{01}^{\mathbf{GCO}}$ describes the contribution resulting from the interaction of the two fragments.

The normal mode motion was also analysis be computing the percent localisation of the mode motion on the two CO fragments:

$$\Lambda^{\mathbf{X}}(j) = \frac{\sum_{\sigma=1}^{N^{\mathbf{X}}} \left|\vec{Q}^{\sigma}(j)\right|}{\sum_{\lambda=1}^{N} \left|\vec{Q}^{\lambda}(j)\right|} \tag{4}$$

where $\left|\vec{Q}^{\lambda}(j)\right|$ is the length of the nuclear displacement vector $\vec{Q}^{\lambda}(j)$ (i.e. the eigenvectors of the mass-weighted Hessian) associated with atoms λ and the normal mode j, N the total number of atoms, $N^{\mathbf{X}}$ the total number of atoms in fragment $\mathbf{X}$.

Tables III–VI list the results of the GCO analysis performed using the CO fragments defined in Fig. 2.

[Figure 2 about here.]

[Table 3 about here.]

[Table 4 about here.]

[Table 5 about here.]

[Table 6 about here.]

List of Figures

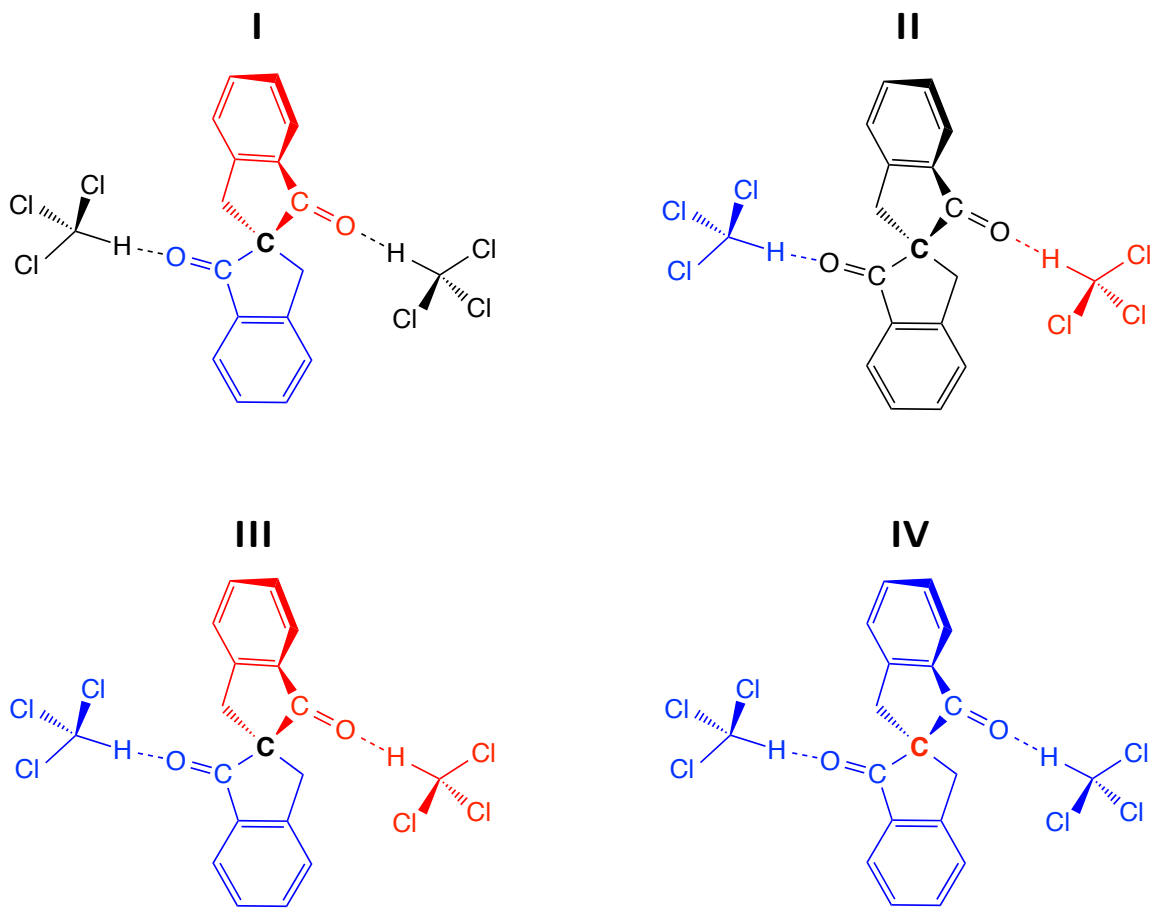

Figure 1: Definitions of the molecular fragments used in the GCO analysis of the modes of the molecular complex formed between one (R)-2,2'-spirobi[indene]-1,1'(3H,3'H)-dione molecule and two chloroform solvent molecules. The CO fragments have been highlighted in red (fragment **A**) and blue (fragment **B**), while the atoms in fragment **R** in black.

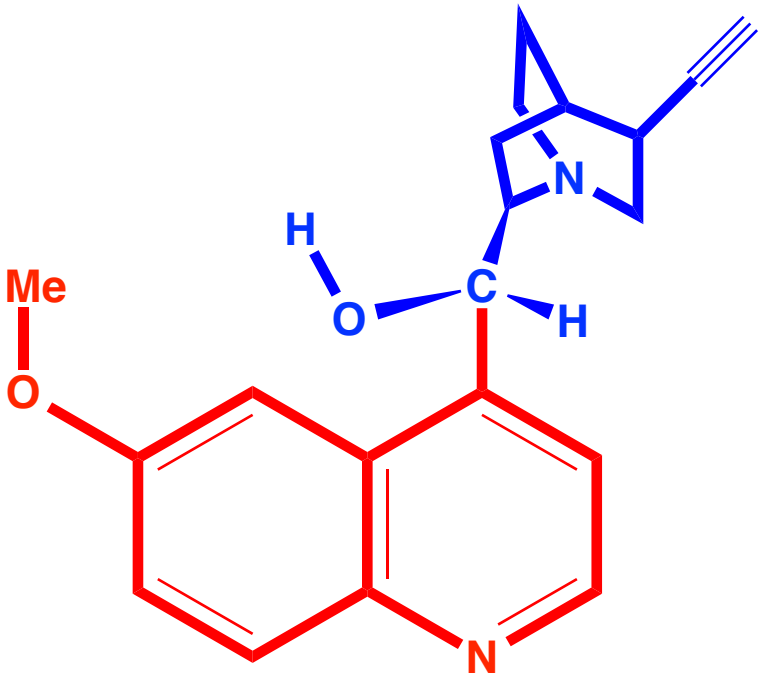

Figure 2: Definitions of the molecular fragments used in the GCO analysis performed for all dehydroquinidine modes. The CO fragments have been highlighted in red (fragment **A**) and blue (fragment **B**).

List of Tables

Frag.	Mode	Freq.	R_{01}	R_{01}^{GCO}	R_{01}^{IF}	R_{01}^{R}	R_{01}^{CO}	R_{01}^{CCO}
I	9	4.5	−0.13	−2.3	+2.4	−0.2	−0.0	−2.3
I	10	7.7	+2.36	+0.5	+0.4	+1.4	+0.1	+0.5
I	11	10.8	+1.06	−0.5	+0.9	+0.6	+0.0	−0.6
I	12	19.9	−4.66	+8.5	+11.2	−24.4	−2.7	+11.1
I	13	24.1	−0.11	−2.7	−1.2	+3.9	+0.8	−3.5
I	14	26.5	−9.78	−2.8	−1.1	−5.9	−0.6	−2.2
I	15	27.5	−5.65	−2.5	+0.9	−4.0	+0.5	−3.0
I	16	32.6	+6.45	+0.0	+1.0	+5.4	−0.1	+0.1
I	17	35.1	+0.98	−1.1	−0.3	+2.4	+0.1	−1.2
I	18	40.0	+1.80	−0.3	−7.3	+9.3	−0.3	+0.0
I	19	49.6	−13.80	−4.2	−4.0	−5.6	+2.2	−6.3
I	20	58.8	+26.02	−3.3	−4.1	+33.5	−5.2	+1.9
I	21	100.1	−1.97	+8.0	−10.3	+0.3	+0.7	+7.3
I	22	128.8	+4.20	+4.6	+1.1	−1.5	−8.6	+13.1
I	23	145.4	−5.69	−4.1	−4.3	+2.8	+7.6	−11.7
I	24	191.2	−5.35	−3.2	−6.8	+4.6	−3.2	−0.0
I	25	199.6	+3.64	+0.2	+0.8	+2.6	+1.6	−1.4
I	26	234.5	−6.31	14.5	−18.6	−2.2	−0.3	+14.7
II	27	245.8	−0.09	+0.1	−0.2	−0.0	−0.3	+0.4
II	28	245.8	−0.59	−0.1	−0.2	−0.2	+0.3	−0.4
II	29	246.3	+0.41	+0.2	+0.3	−0.2	+0.0	+0.2
II	30	246.3	+0.07	−0.2	+0.3	−0.0	−0.0	−0.2
I	31	260.4	+40.38	+2.1	+28.0	+10.4	−2.2	+4.3
I	32	274.4	+23.90	+5.8	+17.0	+1.0	+11.0	−5.2
I	33	283.0	−81.43	−37.1	−30.9	−13.4	+0.5	−37.6
I	34	306.4	+21.42	+13.0	+8.7	−0.3	−0.6	+13.6
II	35	349.6	+4.28	+1.4	+0.6	+2.2	+0.4	+1.1
II	36	349.8	−1.14	−1.4	+0.6	−0.3	−0.4	−1.0
I	37	401.3	−27.63	−19.5	+3.4	−11.6	−4.4	−15.1
I	38	410.1	+29.59	+34.1	−5.9	+1.5	+9.7	+24.3
I	39	458.3	+5.16	+2.5	+12.3	−9.6	−13.2	+15.6
I	40	466.9	−1.35	−3.6	+3.1	−0.8	+5.1	−8.7
I	41	501.0	−32.43	−5.5	−6.0	−21.0	+0.6	−6.1
I	42	511.1	−1.16	−1.3	−20.1	+20.2	−1.4	+0.1
I	43	547.8	+29.35	+30.5	−1.3	+0.1	−7.6	+38.1
I	44	548.1	−7.37	−2.6	+11.9	−16.6	+3.2	−5.8
I	45	580.4	+52.98	+23.1	+36.1	−6.2	−4.5	+27.6
I	46	585.0	−0.88	−0.3	−2.4	+1.9	+0.3	−0.6
III	47	636.7	+21.57	−0.0	+26.1	−4.5	−18.9	+18.9
II	48	637.8	+34.17	+25.8	+7.8	+0.6	+21.2	+4.6
I	49	660.7	+2.86	+3.2	−15.2	+14.8	+3.8	−0.6
I	50	671.9	+34.58	−6.0	−22.8	+63.4	+0.8	−6.8
II	51	681.4	−468.78	−411.9	+33.7	−90.6	−418.2	+6.3
II	52	682.1	+522.89	+482.1	+33.8	+6.9	+489.5	−7.3
I	53	686.1	−5.08	−5.2	+0.3	−0.2	+0.2	−5.4
III	54	695.7	−499.83	−464.4	−35.0	−0.4	−221.3	−243.1
III	55	696.5	+440.00	+500.3	−64.8	+4.5	+274.6	+225.7
I	56	700.7	−31.68	+3.0	−4.9	−29.7	+8.2	−5.3
I	57	701.9	−160.89	−108.3	−3.3	−49.3	−41.3	−67.0
I	58	734.0	+186.53	+222.3	−0.2	−35.5	+138.3	+84.0
I	59	750.0	−119.14	−168.1	+45.1	+3.8	−92.6	−75.5
I	60	778.4	+2.80	−5.3	+5.1	+3.1	−11.2	+5.9
I	61	803.2	+37.96	+44.0	−6.8	+0.7	+8.3	+35.8
I	62	820.4	+0.10	+0.4	−0.5	+0.2	−0.0	+0.4
I	63	822.4	+7.97	−8.1	+4.5	+11.6	−2.0	−6.1
I	64	853.5	−3.95	−1.5	−1.3	−1.1	−0.4	−1.1
I	65	861.6	+0.26	−6.4	+6.3	+0.4	+3.1	−9.5
I	66	893.5	−256.60	−129.5	−114.9	−12.2	+19.8	−149.4

Table I: GCO analysis for modes 9 to 66 of the molecular complex formed between one (R)-2,2'-spirobi[indene]-1,1'(3H,3'H)-dione molecule and two chloroform solvent molecules. The GCO fragments (Frag.) are defined in Fig. 1. Units: cm^{-1} (Freq.), 10^{-44} $esu^2 \cdot cm^2$ (R_{01} and its contributions).

Frag.	Mode	Freq.	R_{01}	R_{01}^{GCO}	R_{01}^{IF}	R_{01}^{R}	R_{01}^{CO}	R_{01}^{CCO}
I	67	900.4	−6.69	+32.9	−36.4	−3.1	+0.0	+32.9
I	68	935.2	+20.73	+12.1	+7.5	+1.2	−12.1	+24.1
I	69	939.4	+14.36	+2.0	+4.0	+8.3	−0.1	+2.1
I	70	945.9	+36.95	+2.3	+36.5	−1.8	−5.9	+8.2
I	71	972.4	+0.12	−0.7	−0.0	+0.8	−0.1	−0.5
I	72	972.5	+0.42	+0.5	−0.0	−0.0	+0.1	+0.4
IV	73	986.8	+186.93	+91.2	+90.1	+5.7	−2.6	+93.8
I	74	1012.7	−3.42	−1.4	−0.1	−1.9	−0.4	−1.0
I	75	1013.3	+0.38	+0.5	−0.2	+0.0	+0.4	+0.2
I	76	1042.7	−2.22	+17.1	−22.7	+3.4	+0.0	+17.1
I	77	1084.6	+0.86	−8.0	−1.8	+10.6	+1.1	−9.1
I	78	1087.9	+7.89	+0.3	+6.1	+1.4	−1.5	+1.8
I	79	1117.9	+8.67	+7.1	−1.8	+3.4	−1.8	+8.9
I	80	1142.7	+14.51	+13.1	−1.7	+3.1	+6.1	+7.0
I	81	1143.0	−18.39	−11.3	−7.6	+0.5	−6.2	−5.1
I	82	1170.0	+1.58	−6.8	+7.8	+0.6	−2.4	−4.5
I	83	1170.8	−6.69	+4.6	−7.6	−3.7	+0.9	+3.7
I	84	1178.4	−14.42	−8.2	−0.7	−5.5	+1.5	−9.7
IV	85	1193.6	+88.36	+69.0	+17.1	+2.3	+8.3	+60.7
I	86	1198.9	−8.94	+8.6	−3.7	−13.9	+2.7	+6.0
I	87	1199.3	−30.50	−16.0	−9.3	−5.2	−6.4	−9.6
II	88	1212.3	−81.70	−91.4	+4.5	+5.2	−98.3	+6.8
II	89	1212.3	+90.49	+89.1	+4.6	−3.2	+96.0	−6.9
II	90	1217.1	+100.38	+91.1	+7.1	+2.1	+89.6	+1.6
II	91	1217.2	−72.98	−88.7	+6.6	+9.1	−87.2	−1.5
I	92	1247.5	−187.58	−67.2	−40.8	−79.6	+9.9	−77.1
I	93	1261.5	+25.31	+77.1	−52.4	+0.6	+3.9	+73.2
I	94	1283.9	−7.70	−5.2	−0.1	−2.4	−1.8	−3.4
I	95	1287.0	+38.54	+11.9	+3.9	+22.8	+5.6	+6.3
I	96	1352.7	+10.08	+30.7	−21.8	+1.2	+9.7	+21.0
I	97	1355.8	−65.26	−38.1	−28.2	+1.1	−15.7	−22.3
I	98	1414.9	+0.16	−7.6	+8.8	−1.1	−13.0	+5.4
I	99	1416.0	+76.49	+52.7	+21.3	+2.6	+50.6	+2.1
I	100	1448.4	+32.53	+24.8	+7.2	+0.5	+2.6	+22.2
I	101	1448.5	−6.80	−9.6	+3.1	−0.4	+2.5	−12.1
I	102	1457.5	−36.71	−41.8	+5.0	+0.1	−15.5	−26.4
I	103	1457.7	+30.37	+30.2	+1.8	−1.6	+10.3	+19.8
I	104	1574.8	+35.29	+29.0	+13.5	−7.2	+21.2	+7.8
I	105	1575.6	−8.77	−18.6	+9.5	+0.3	−15.7	−2.9
I	106	1589.4	−30.09	−16.1	−16.6	+2.6	+2.2	−18.2
I	107	1590.5	−1.28	+16.2	−17.4	−0.0	−4.4	+20.6
I	108	1671.6	+867.96	+723.2	+224.3	−79.6	+635.2	+88.0
I	109	1696.9	−521.13	−766.3	+253.3	−8.1	−704.7	−61.7
I	110	2961.5	−0.34	−8.6	+8.1	+0.2	+5.3	−14.0
I	111	2965.1	+16.34	+8.9	+7.6	−0.2	−4.8	+13.7
I	112	3011.7	−2.87	−1.2	−1.9	+0.2	+1.7	−2.9
I	112	3011.7	−2.87	−1.2	−1.9	+0.2	+1.7	−2.9
I	113	3013.1	−0.16	+2.0	−2.2	+0.0	−0.5	+2.6
II	114	3073.7	+70.19	+43.0	+37.1	−9.9	+4.0	+39.0
II	115	3074.2	−4.72	−43.0	+37.0	+1.3	−4.0	−39.0
I	116	3097.4	+0.29	+0.8	−0.5	−0.0	+1.4	−0.6
I	117	3097.4	−1.10	−0.8	−0.5	+0.2	−1.4	+0.6
I	118	3107.4	+7.03	+9.1	−2.6	+0.5	+6.2	+2.9
I	119	3107.5	−11.16	−9.0	−2.6	+0.5	−6.1	−2.9
I	120	3116.1	+5.56	+6.5	−0.9	+0.0	+7.9	−1.4
I	121	3116.1	−7.38	−6.6	−0.9	+0.2	−8.1	+1.4
I	122	3125.1	−4.19	−2.1	−2.4	+0.4	+2.4	−4.6
I	123	3125.2	−0.41	+2.3	−2.4	−0.3	−2.4	+4.7

Table II: GCO analysis for modes 67 to 123 of the molecular complex formed between one (R)-2,2'-spirobi[indene]-1,1'(3H,3'H)-dione molecule and two chloroform solvent molecules. The GCO fragments (Frag.) are defined in Fig. 1. Units: cm^{-1} (Freq.), 10^{-44} $esu^2 \cdot cm^2$ (R_{01} and its contributions).

Frag.	Freq.	R_{01}	R_{01}^{GCO}	R_{01}^{IF}	$\Lambda^{\mathbf{A}}$	$\Lambda^{\mathbf{B}}$	Total
8	19.8	−1.0	−4.9	+3.9	40.2	59.8	100.0
9	35.9	+6.6	+2.3	+4.3	47.5	52.5	100.0
10	48.1	−7.4	−0.5	−6.9	46.0	54.0	100.0
11	70.1	−1.2	+2.8	−4.1	57.9	42.1	100.0
12	127.8	+4.2	+1.4	+2.8	37.8	62.2	100.0
13	131.0	+4.4	+1.9	+2.5	74.5	25.5	100.0
14	134.2	12.7	+5.6	+7.1	28.3	71.7	100.0
15	151.2	−2.7	+1.2	−3.9	38.6	61.4	100.0
16	156.6	−2.1	+1.3	−3.4	40.1	59.9	100.0
17	194.4	+70.9	+81.0	−10.1	48.2	51.8	100.0
18	206.8	+4.3	−3.4	+7.7	46.5	53.5	100.0
19	209.9	−88.0	−87.3	−0.7	51.1	48.9	100.0
20	219.0	−13.7	−14.3	+0.6	65.9	34.1	100.0
21	222.0	−15.4	−7.3	−8.1	17.9	82.1	100.0
22	249.9	+2.1	+4.1	−2.0	45.4	54.6	100.0
23	297.4	+14.7	+11.1	+3.6	41.9	58.1	100.0
24	307.6	+1.4	−0.7	+2.2	34.6	65.4	100.0
25	331.6	+0.1	−2.6	+2.7	16.4	83.6	100.0
26	333.9	+7.3	+3.9	+3.4	46.3	53.7	100.0
27	361.8	−11.0	−11.4	+0.4	55.3	44.7	100.0
28	369.4	+8.6	+12.5	−3.9	28.5	71.5	100.0
29	403.7	−4.9	−5.0	+0.2	42.7	57.3	100.0
30	406.2	+5.2	+13.2	−8.0	35.9	64.1	100.0
31	443.6	−6.9	−3.1	−3.8	50.9	49.1	100.0
32	458.2	+13.8	+5.7	+8.0	51.5	48.5	100.0
33	492.5	+12.2	−0.9	+13.1	29.2	70.8	100.0
34	496.7	−11.9	−6.7	−5.2	61.8	38.2	100.0
35	521.0	−11.5	−11.7	+0.1	40.4	59.6	100.0
36	536.2	−29.9	−6.3	−23.7	71.7	28.3	100.0
37	539.4	+43.3	+7.9	+35.3	81.3	18.7	100.0
38	553.6	−4.4	+5.0	−9.4	27.4	72.6	100.0
39	573.7	−13.3	−1.1	−12.2	10.3	89.7	100.0
40	589.9	−3.4	−1.3	−2.2	60.1	39.9	100.0
41	605.0	+79.6	+28.3	+51.3	28.2	71.8	100.0
42	608.2	−33.6	−4.1	−29.5	13.1	86.9	100.0
43	621.2	+67.1	+14.6	+52.4	33.5	66.5	100.0
44	629.5	−66.8	−5.8	−60.9	14.5	85.5	100.0

Table III: GCO analysis for modes 8 to 44 of dehydroquinidine. The GCO fragments (Frag.) are defined in Fig. 1. Units: cm^{-1} (Freq.), 10^{-44} $esu^2 \cdot cm^2$ (R_{01} and its contributions).

Frag.	Freq.	R_{01}	R_{01}^{GCO}	R_{01}^{IF}	$\Lambda^{\mathbf{A}}$	$\Lambda^{\mathbf{B}}$	Total
45	673.8	+3.0	−0.3	+3.4	69.4	30.6	100.0
46	690.7	+1.3	−2.6	+3.9	72.6	27.4	100.0
47	730.4	−9.0	−12.2	+3.2	49.2	50.8	100.0
48	740.3	−61.2	−9.5	−51.6	22.1	77.9	100.0
49	769.0	−0.7	+1.2	−2.0	77.7	22.3	100.0
50	790.3	−43.5	+2.6	−46.1	17.8	82.2	100.0
51	803.5	+74.4	+2.6	+71.8	7.2	92.8	100.0
52	810.5	+14.1	+5.5	+8.6	73.4	26.6	100.0
53	827.4	−83.0	−74.6	−8.5	41.7	58.3	100.0
54	837.7	+1.2	−9.8	+11.0	37.8	62.2	100.0
55	838.4	+1.7	+4.5	−2.8	57.5	42.5	100.0
56	846.4	+58.0	+53.7	+4.3	36.6	63.4	100.0
57	865.5	−25.3	−14.1	−11.2	49.6	50.4	100.0
58	899.8	+26.3	+27.8	−1.4	43.7	56.3	100.0
59	906.5	−23.3	−16.6	−6.7	35.4	64.6	100.0
60	909.8	−15.1	−15.6	+0.5	15.3	84.7	100.0
61	938.9	+0.1	+1.2	−1.1	74.3	25.7	100.0
62	943.1	−0.4	−1.2	+0.8	18.2	81.8	100.0
63	944.8	−0.5	+1.0	−1.5	76.3	23.7	100.0
64	962.1	+29.2	−11.7	+41.0	11.0	89.0	100.0
65	984.3	−22.5	+4.4	−26.9	10.5	89.5	100.0
66	988.3	+55.6	−40.5	+96.1	33.1	66.9	100.0
67	1003.3	+75.4	+94.7	−19.3	73.7	26.3	100.0
68	1007.1	−55.0	−22.2	−32.8	32.6	67.4	100.0
69	1013.4	−1.3	−0.1	−1.2	29.7	70.3	100.0
70	1030.5	+72.9	−12.8	+85.8	28.8	71.2	100.0
71	1038.6	+4.5	−1.0	+5.5	14.3	85.7	100.0
72	1062.0	−46.6	−14.3	−32.2	15.4	84.6	100.0
73	1074.7	−13.4	−0.1	−13.4	43.9	56.1	100.0
74	1082.1	−38.9	−41.5	+2.6	30.8	69.2	100.0
75	1113.3	+16.0	+12.9	+3.1	20.8	79.2	100.0
76	1120.5	+25.7	+23.8	+1.9	69.3	30.7	100.0
77	1126.4	+1.6	−0.4	+2.0	95.5	4.5	100.0
78	1134.1	+20.2	+20.2	+0.0	8.8	91.2	100.0
79	1159.3	+246.9	+228.4	+18.5	65.0	35.0	100.0
80	1173.4	+33.0	+57.4	−24.4	21.3	78.7	100.0
81	1179.6	+323.0	+314.1	+8.8	51.7	48.3	100.0

Table IV: GCO analysis for modes 45 to 64 of dehydroquinidine. The GCO fragments (Frag.) are defined in Fig. 1. Units: cm^{-1} (Freq.), 10^{-44} $esu^2 \cdot cm^2$ (R_{01} and its contributions).

Frag.	Freq.	R_{01}	R_{01}^{GCO}	R_{01}^{IF}	$\Lambda^{\mathbf{A}}$	$\Lambda^{\mathbf{B}}$	Total
82	1194.4	−73.1	−86.5	+13.4	24.9	75.1	100.0
83	1205.6	−499.2	−447.6	−51.6	29.2	70.8	100.0
84	1215.9	−100.0	−88.9	−11.1	43.1	56.9	100.0
85	1224.3	−23.8	−14.2	−9.6	27.3	72.7	100.0
86	1231.7	+46.5	+56.2	−9.6	64.7	35.3	100.0
87	1234.1	+12.0	+6.0	+6.0	3.5	96.5	100.0
88	1249.2	−7.5	−6.9	−0.6	64.2	35.8	100.0
89	1260.1	−11.4	0.2	−11.6	21.1	78.9	100.0
90	1278.8	−8.2	−0.5	−7.7	6.1	93.9	100.0
91	1291.5	−19.3	−8.0	−11.3	11.4	88.6	100.0
92	1294.6	+9.2	−2.4	+11.5	13.0	87.0	100.0
93	1298.2	−13.9	−6.4	−7.6	18.4	81.6	100.0
94	1305.1	+14.9	−10.9	+25.8	9.4	90.6	100.0
95	1312.5	−84.5	−59.7	−24.8	37.0	63.0	100.0
96	1315.5	+27.1	+0.1	+27.0	6.1	93.9	100.0
97	1325.3	−13.2	+6.1	−19.3	4.1	95.9	100.0
98	1329.8	+3.5	−3.1	+6.6	4.4	95.6	100.0
99	1341.3	−6.5	−8.4	+1.9	71.6	28.4	100.0
100	1351.4	+34.9	+32.5	+2.4	17.2	82.8	100.0
101	1353.1	+0.9	+2.4	−1.5	85.0	15.0	100.0
102	1382.4	+71.2	+53.3	+17.9	27.2	72.8	100.0
103	1412.7	−8.8	+5.6	−14.4	93.9	6.1	100.0
104	1429.4	−9.0	−4.9	−4.1	90.4	9.6	100.0
105	1435.5	−6.1	+0.3	−6.4	10.0	90.0	100.0
106	1435.7	−4.8	+1.2	−6.0	83.3	16.7	100.0
107	1440.9	−6.7	−15.7	+9.0	10.7	89.3	100.0
108	1441.7	−2.0	−0.4	−1.6	2.1	97.9	100.0
109	1448.0	+17.1	+20.0	−3.0	80.6	19.4	100.0
110	1452.8	−2.5	−0.3	−2.2	6.0	94.0	100.0
111	1455.1	+18.8	+26.6	−7.8	91.7	8.3	100.0
112	1492.6	−18.2	−30.3	+12.1	94.3	5.7	100.0
113	1550.3	−2.7	+4.9	−7.6	92.2	7.8	100.0
114	1571.3	+7.1	+2.8	+4.3	86.7	13.3	100.0
115	1600.6	−28.4	−6.5	−21.8	96.9	3.1	100.0
116	2111.5	+3.4	−0.4	+3.8	0.1	99.9	100.0
117	2917.5	−10.9	−0.0	−10.8	0.3	99.7	100.0

Table V: GCO analysis for modes 82 to 117 of dehydroquinidine. The GCO fragments (Frag.) are defined in Fig. 1. Units: cm^{-1} (Freq.), 10^{-44} $esu^2 \cdot cm^2$ (R_{01} and its contributions).

Frag.	Freq.	R_{01}	R_{01}^{GCO}	R_{01}^{IF}	$\Lambda^{\mathbf{A}}$	$\Lambda^{\mathbf{B}}$	Total
118	2930.8	+1.9	−0.0	+1.9	1.7	98.3	100.0
119	2943.3	+6.3	+0.1	+6.2	0.1	99.9	100.0
120	2951.2	+8.1	−3.2	+11.3	96.3	3.7	100.0
121	2953.4	+12.2	+2.4	+9.8	1.8	98.2	100.0
121	2953.4	+12.2	+2.4	+9.8	1.8	98.2	100.0
122	2965.6	−34.0	+0.8	−34.8	0.2	99.8	100.0
123	2973.2	+4.8	+0.0	+4.8	1.9	98.1	100.0
124	2979.6	+3.4	+0.3	+3.1	0.3	99.7	100.0
125	2991.5	+43.8	−0.2	+43.9	0.1	99.9	100.0
126	2996.6	+33.0	−0.1	+33.1	0.5	99.5	100.0
127	3006.8	−5.4	−0.5	−4.9	0.4	99.6	100.0
128	3013.5	−16.3	+0.1	−16.4	0.6	99.4	100.0
129	3017.7	−7.3	+0.8	−8.1	98.7	1.3	100.0
130	3028.5	+8.8	+0.3	+8.5	0.4	99.6	100.0
131	3081.3	−2.0	−0.6	−1.4	99.0	1.0	100.0
132	3088.0	+0.7	+0.0	+0.7	99.6	0.4	100.0
133	3106.8	+5.5	+0.2	+5.3	98.0	2.0	100.0
134	3111.5	+0.1	−0.0	+0.1	99.9	0.1	100.0
135	3126.1	+0.1	+0.0	+0.1	99.7	0.3	100.0
136	3154.3	+9.4	−0.0	+9.4	97.9	2.1	100.0
137	3372.0	+17.8	−0.1	+17.9	0.0	100.0	100.0
138	3651.0	−12.9	−0.0	−12.9	0.5	99.5	100.0

Table VI: GCO analysis for modes 118 to 138 of dehydroquinidine. The GCO fragments (Frag.) are defined in Fig. 1. Units: cm^{-1} (Freq.), 10^{-44} $esu^2 \cdot cm^2$ (R_{01} and its contributions).